Determination of Optimum Combination of Voxel Size and b-value for Brain Diffusion Tensor Imaging
(Penentuan Gabungan Optimum Saiz Voksel dan Nilai-b untuk Pengimejan Tensor Difusi Otak)

Nur Hartini Mohd Taib*, Wan Ahmad Kamil Wan Abdullah, Ibrahim Lutfi Shuaib,
Enrico Magosso & Suzana Mat Isa

ABSTRACT

Optimum combination of voxel size resolution and b-value for whole brain imaging has been determined. Data images were acquired using a 1.5T magnetic resonance imaging (MRI) system (GE Signa HDxt). Diffusion tensor imaging (DTI) scan was performed on phantom and a human volunteer. Six protocols which consist of various combination of voxel size and b-value were evaluated. Measurement of signal-to-noise ratio (SNR) and DTI parameter indices were carried out for both phantom and in-vivo studies. Due consideration was given to a combination of parameters yielding sufficient SNR with DTI values comparable to those obtained from previous reported studies. For the phantom study, SNR ≥ 20 was found in all of the protocols except for a combination of voxel size of $2.0 \times 2.0 \times 2.0$ mm^3 with b-value of 1200 s/mm^2 (V2.0 B1200) and that of voxel size of $2.0 \times 2.0 \times 2.0$ mm^3 with b-value of 1000 s/mm^2 (V2.0 B1000). For in-vivo study, all protocols presented SNR > 20. It was found that a combination of voxel size of $2.5 \times 2.5 \times 2.5$ mm^3 with b-value of 1000 s/mm^2 (V2.5 B1000) and that of voxel size of $2.5 \times 2.5 \times 2.5$ mm^3 with b-value of 700 s/mm^2 (V2.5 B700) displayed the most comparable ADC and FA values with references. In terms of anatomic coverage, V2.5 B700 was found better than V2.5 B1000 as it assures coverage of the whole brain. In conclusion, a combination of voxel size of $2.5 \times 2.5 \times 2.5$ mm^3 with b-value of 700 s/mm^2 was considered as optimum parameters for brain DTI.

Keywords: Brain imaging; b-value; diffusion tensor imaging; optimization; voxel size

ABSTRAK

Gabungan optimum peleraian saiz voksel dan nilai-b untuk pengimejan seluruh otak telah ditentukan. Data imej telah diperoleh menggunakan sistem pengimejan resonans magnet (MRI) 1.5T (GE Signa HDxt). Imbasan pengimejan tensor difusi (DTI) telah dilakukan ke atas fantom dan seorang sukarelawan. Enam protokol yang terdiri daripada pelbagai gabungan saiz voksel dan nilai-b telah dinilai. Pengukuran nisbah isyarat-hingar (SNR) dan parameter indeks DTI telah dilakukan untuk kajian fantom dan in-vivo. Pertimbangan yang sewajarnya telah diberikan kepada gabungan parameter yang menghasilkan SNR mencukupi dan nilai DTI setara dengan yang diperoleh daripada kajian terdahulu. Untuk kajian fantom, didapati SNR ≥ 20 bagi semua protokol kecuali gabungan saiz voksel $2.0 \times 2.0 \times 2.0$ mm^3 dengan nilai-b 1200 s/mm^2 (V2.0 B1200) dan gabungan saiz voksel $2.0 \times 2.0 \times 2.0$ mm^3 dengan nilai-b 1000 s/mm^2 (V2.0 B1000). Bagi kajian in-vivo, semua protokol menunjukkan SNR > 20. Didapati gabungan saiz voksel $2.5 \times 2.5 \times 2.5$ mm^3 dengan nilai-b 1000 s/mm^2 (V2.5 B1000) dan saiz voksel $2.5 \times 2.5 \times 2.5$ mm^3 dengan nilai-b 700 s/mm^2 (V2.5 B700) telah mempamerkan nilai ADC dan FA paling setara dengan rujukan. Daripada segi liputan anatomi, didapati V2.5 B700 lebih baik daripada V2.5 B1000 kerana ia menjamin liputan seluruh otak. Kesimpulannya, gabungan saiz voxel $2.5 \times 2.5 \times 2.5$ mm^3 dengan nilai-b 700 s/mm^2 dianggap sebagai parameter yang optimum untuk DTI otak.

Kata kunci: Nilai-b; pengimejan otak; pengimejan tensor difusi; pengoptimuman; saiz voksel

INTRODUCTION

Recently, diffusion tensor imaging (DTI) has become established as a tool for brain imaging. DTI measures signal attenuation from diffusion of water molecules present in brain tissues and has many advantages over other conventional magnetic resonance imaging (MRI) techniques as it gives tissue information at macro and micro structural level. The example of parameter indices derived from DTI are apparent diffusion coefficient (ADC) or mean diffusivity (MD) which characterises molecular diffusivity and fractional anisotropy (FA) which quantitatively describes molecular diffusivity variation in different directions (Jones et al. 1999; Le Bihan et al. 2001). Moreover, by using DTI technique, visualisation of white matter tracts architecture is available, which opened doors to inspection of microstructural integrity and connectivity of normal and diseased white matter neuronal fibres (Chanraud et al. 2010; Madden et al. 2009).

However, the anisotropy indices are dependent on signal-to-noise ratio (SNR) (Mori 2007; Mukherjee et al. 2008a). Several imaging parameters influencing SNR of magnetic resonance images are described by the equation:

$$SNR \propto \left(\frac{FOV_x}{N_x} . \frac{FOV_y}{N_y} . \Delta Z \right) \times \sqrt{\frac{N_x . N_y . NEX}{RBW}} , \qquad (1)$$

where FOV_x and FOV_y are field-of-view in phase- and frequency-directions, respectively, N_x and N_y are the number of phase- and frequency-encoding matrix, respectively, ΔZ is slice thickness, NEX is number of signal averaging, and RBW is the receiver bandwidth (McRobbie et al. 2006).

In addition to ordinary MRI parameters, the SNR of DTI images are also influenced by its sequence-specific imaging parameters. In DTI images, the signal is measured using signal attenuation which is exponentially correlated with b-value as described in (2). An increase in b-value results in reduction of SNR (Alexander & Barker 2005).

$$\frac{S}{S_o} = e^{-bD}, \qquad (2)$$

where S and S_o are signal intensity of diffusion- and non-diffusion-weighted magnetization, respectively; b is b-value; and D is diffusion coefficient. If parallel imaging technique is used, SNR of accelerated images (SNR_R) reduces due to decrease of data sampling and increase of noise in the image (3) (Reeder et al. 2005).

$$SNR_R = \frac{SNR_o}{g\sqrt{R}}, \qquad (3)$$

where SNR_o is SNR of an equivalent unaccelerated image; g is g-factor; and R (≥ 1) is the acceleration factor used during acquisition.

Even though many studies employing DTI are present in literature, until now there has been no specific optimized protocols standardized for a multitude of applications. Optimization requires consideration of four main factors: MRI hardware configuration, available scanning time, anatomic coverage needed and specific anatomic structure to be investigated (Mukherjee et al. 2008a).

Therefore, the aim of the present study was to determine the optimum combination of b-value and voxel size. In order to obtain the optimal parameters, assessment was performed on the SNR and then ADC and FA values of the data images. Due consideration was given to a combination of parameters yielding sufficient SNR as well as DTI values which are comparable to those obtained from previous reported studies (Alexander & Barker 2005; Hunsche et al., 2001; Laganà et al. 2010; Lazar & Alexander 2003; Löbel et al. 2009). The present investigation was performed on phantom and human volunteer.

MATERIALS AND METHODS

SUBJECTS

Phantom   A standard spherical TLT head phantom with diameter of 170 mm (GE Healthcare) was used. It was kept in the MRI scanner room all the time and at scanning time, the temperature of phantom was recorded, that was 20°C.

Human volunteer   A healthy female volunteer aged 30.5 years participated in the study. The subject never had any brain injury, neurological or psychiatric illness. The subject signed an informed consent form in compliance with the regulations of the institutional ethics committee.

MR IMAGING

Phantom study   The phantom was placed in an eight-channel neurovascular array (NVA) coil for scanning. DTI data were acquired using a 1.5T MRI system (GE Signa HDxt) with maximum gradient amplitude of 33 mT/m. The voxel size resolution was varied at $2.0 \times 2.0 \times 2.0$ mm^3 and $2.5 \times 2.5 \times 2.5$ mm^3 and the b-value was varied at 700, 1000 and 1200 s/mm^2. Array Spatial Sensitivity Encoding Technique (ASSET) parallel imaging technique was utilized in the study (King 2004). All other scan parameters were fixed to a specific value, as described in Tables 1 and 2. The whole scan consist of six protocols and the entire scan was repeated three times for reproducibility study. While repeating the scanning, the second and the third scan were performed after 1 h interval to allow the temperature of phantom and scanner cooled down to their initial state. This is to minimize the effect of radio frequency heating on phantom which will affect the ADC and FA values acquired.

In-vivo study   During *in-vivo* study, subject's head was placed in the same NVA coil. The scanning was carried out for all protocols listed in Table 2. No scan repetition was performed as it is unnecessary and unpractical, as discussed further in the *Limitations and recommendation for future work* section.

DATA ANALYSIS

All data images were transferred to an independent workstation for post processing. SNR and diffusion parameter indices were measured using preinstalled software, Advance Workstation viewer version 4.3 and Functool version 4.5.1 with Fibertrak option (GE Medical Systems), respectively.

Measurement of signal-to-noise ratio   For the phantom data, SNR was measured on the centre slice of b$_o$ images of phantom. One circular region of interest (ROI) with diameter of 15 cm was placed at the centre of the image, covering at least 75% of the phantom area. As for *in-vivo* study, SNR was also measured on b$_o$ images of the data. ROI was located on the axial slice at the horizontal level of the striatum containing genu and splenium of the corpus callosum. A square ROI of 16.0 ± 2.0 mm^2 was drawn manually in right and left white matter (WM) and grey matter (GM) areas, as described previously (Mohd Taib et al. 2012). SNR measured at all ROIs in respective white and grey matter was averaged out. ROIs were also placed in region of cerebrospinal fluid (CSF) at another different slice

TABLE 1. The imaging parameters which were kept fixed for all of the protocols

Parameters	Values
Pulse sequence	Single shot spin echo, echo planar imaging
Echo time, TE (ms)	(minimum) subject to b-value
No. of diffusion directions	30
No. of unweighted images	3
ASSET acceleration factor	2
Phase-encoding direction	R/L
Inter-slice spacing	0
Receiver bandwidth, RBW (Hz)	1953.12
Number of signal averaging, NEX	1

TABLE 2. The imaging parameters that were altered according to the six protocols assessed

Parameters		Voxel size	
		2.0 mm^3	2.5 mm^3
Repetition time, TR (ms)		17 000	13 000
Field-of-view, FOV (mm$^{2)}$)		256 × 256	240 × 240
Matrix		128 × 128	96 × 96
Slice thickness (mm)		2.0	2.5
b-value (s/mm^2)	1200	Protocol 1: V2.0 B1200	Protocol 4: V2.5 B1200
	1000	Protocol 2: V2.0 B1000	Protocol 5: V2.5 B1000
	700	Protocol 3: V2.0 B700	Protocol 6: V2.5 B700

containing the body of lateral ventricles. ROI was located similar to reference for comparison purposes (Ding et al. 2007). For both phantom and *in-vivo* study, measurement was made in first and second volume of b$_o$ images and SNR was calculated using the difference method as proposed by previous studies on influence of parallel imaging technique on SNR of MRI images (Dietrich et al. 2007).

Measurement of DTI parameter indices   ADC and FA values for all protocols were measured at the same ROI as described previously. The results were compared to previous work which used similar 1.5T MRI system (Alexander & Barker 2005; Hunsche et al. 2001; Löbel et al. 2009). The comparisons are in the form of percentage difference which was calculated as,

$$Percentage\ of\ difference\ (\%) = \frac{X_f - X_h}{X_h} \times 100, \qquad (4)$$

$$Percentage\ of\ difference\ (\%) = \frac{X_l - X_f}{X_l} \times 100, \qquad (5)$$

where X_f is current finding; X_h is highest value from reference; and X_l is lowest value from reference. In the case of current findings are higher than that of highest value from reference, (4) was used, whereas if current findings are less than the lowest value from reference, (5) was used.

STATISTICAL ANALYSIS

Independent t-test was used to perform the statistical analysis for comparison of SNR between protocols for phantom and *in-vivo* study, as well as for comparison of ADC and FA values for phantom study. A 2-tailed, *p*<0.05 was considered significant.

RESULTS

PHANTOM STUDY

Figure 1 presents the SNR value measured on phantom images. All protocols listed in Table 2 showed SNR ≥ 20 except V2.0 B1200 (mean ± standard deviation; 18.83 ± 2.49) and V2.0 B1000 (19.66 ± 1.36). All combinations of voxel size 2.5 × 2.5 × 2.5 mm^3 with respective b-value showed SNR relatively two-fold higher than that of voxel size 2.0 × 2.0 × 2.0 mm^3 (*p*<0.05). Meanwhile, although there are trend of SNR increasing with reduction of b-value between similar voxel size, there are no any significant difference was noted. Variance and standard deviation between three measurements was found small.

Figure 2 demonstrates ADC and FA values measured on phantom images. All protocols displayed very slight difference in ADC value with percentage difference ranging from 0.25 to 6.16%. However, the only protocol that displayed significant difference compared to all other protocols is V2.0 B1200. On the other hand, moderate to high variation in FA values exhibited by all protocols (range from 7.08 to 127.59%) achieved significant different. However, a comparison between V2.0 B1200-V2.0 B1000, V2.0 B700-V2.5 B1200, and V2.5 B1000-V2.5 B700 was found insignificant. High standard deviation and variance of ADC and FA values
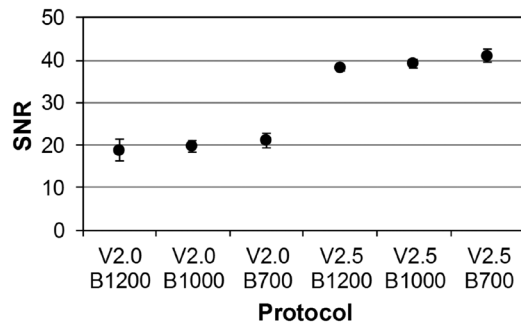
FIGURE 1. The SNR values of phantom for specific combination of voxel size and b-value. Except for the protocols of V2.0 B1200 and V2.0 B1000, the SNR value showed greater than 20. The error bars indicate the standard deviation between three measurements
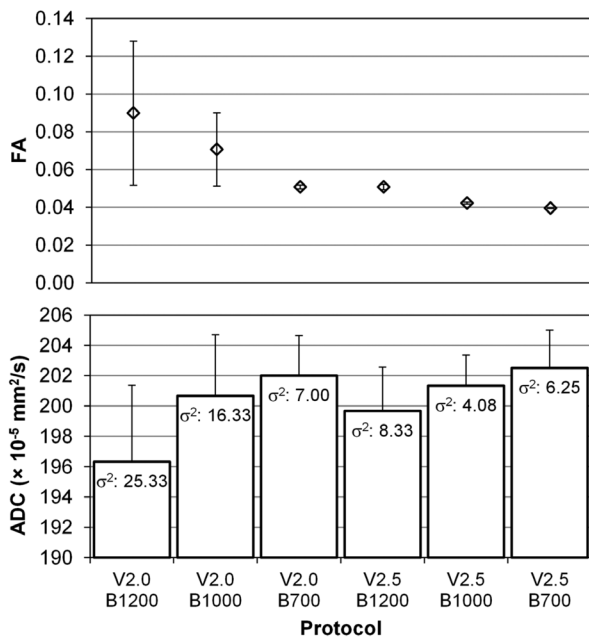

FIGURE 2. The mean and standard deviation of ADC and FA values measured on the phantom images

were also noted in V2.0 B1200 while moderate of that were seen in V2.0 B1000. It is also noted that V2.0 B700 and V2.5 B700 displayed a comparable ADC values that are $(202.00\pm2.65) \times 10^{-5}$ mm^2/s and $(202.50\pm2.50) \times 10^{-5}$ mm^2/s, respectively. However, V2.0 B700 showed a higher FA value, that is $(5.08\pm0.10) \times 10^{-2}$ compared to V2.5 B700, that is $(3.95\pm0.02) \times 10^{-2}$.

IN-VIVO STUDY

As Figure 3 depicts, all protocols showed SNR of CSF > 20, which range from 25.45 to 44.26. However only V2.5 B1200 displayed significantly higher SNR compared to that of all protocols with voxel size 2.0 × 2.0 × 2.0 mm^3. Meanwhile, all combination of voxel size 2.5 × 2.5 × 2.5 mm^3 with their respective b-values displayed a fairly but insignificantly higher SNR of WM and GM compared to
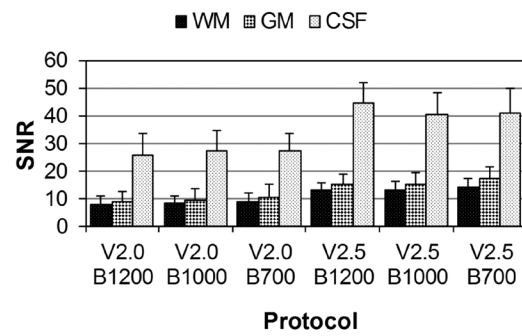

FIGURE 3. The SNR values measured at WM, GM, and CSF areas of human brain

that of voxel size 2.0 × 2.0 × 2.0 mm^3. An insignificantly higher SNR was also noted in GM compared to WM for each of the protocol.

Figure 4 illustrates the ADC and FA values obtained from *in-vivo* study while Figure 5 presents the percentage difference from the references. In Figure 5, the bars show differences at each ROI for all protocols. Values that matched with previous studies are indicated as 0% differed from references.

From Figure 4, it is noticed that protocols with larger voxel size and smaller b-value produced more comparable results to references. As described in Figure 5(a), protocols that exhibited ADC values with smallest percentage difference compared to previous studies were V2.5 B1000 and V2.5 B700 (3.66-11.13% and 0.49-5.51%, respectively). It can also be seen that V2.0 B1200 and V2.0 B1000 exhibited ADC values which differed considerably from references (6.77-59.18% and 3.40-35.09%, respectively). It was noticed that the difference is obvious mainly in area of genu and splenium. At genu, the greatest difference was 59.18% for V2.0 B1200 and 28.18% for V2.0 B1000, whilst at splenium, the biggest difference was 54.03% and 35.09% for V2.0 B1200 and V2.0 B1000, respectively. Similar outcome was observed for FA values (Figure 5(b)) in which V2.5 B1000 and V2.5 B700 were found least differed to references with percentage of 8.79-19.27% and 4.98-25.55%, respectively, whereas V2.0 B1200 and V2.0 B1000 demonstrated the largest difference (7.96-37.57% and 8.79-47.02%, respectively). In terms of number of ROI, V2.5 B700 was found displaying FA values that matched the references at three ROIs, compared to V2.5 B1000 which shows only two of that.

DISCUSSION

IMAGING PARAMETERS

As in most of MRI procedure, the goal is to obtain data images with good quality at acceptable scan time. The typical imaging parameters include those mentioned in (1) to (3) and as displayed in Tables 1 and 2. In this study, we tried to vary all related imaging parameters that influence
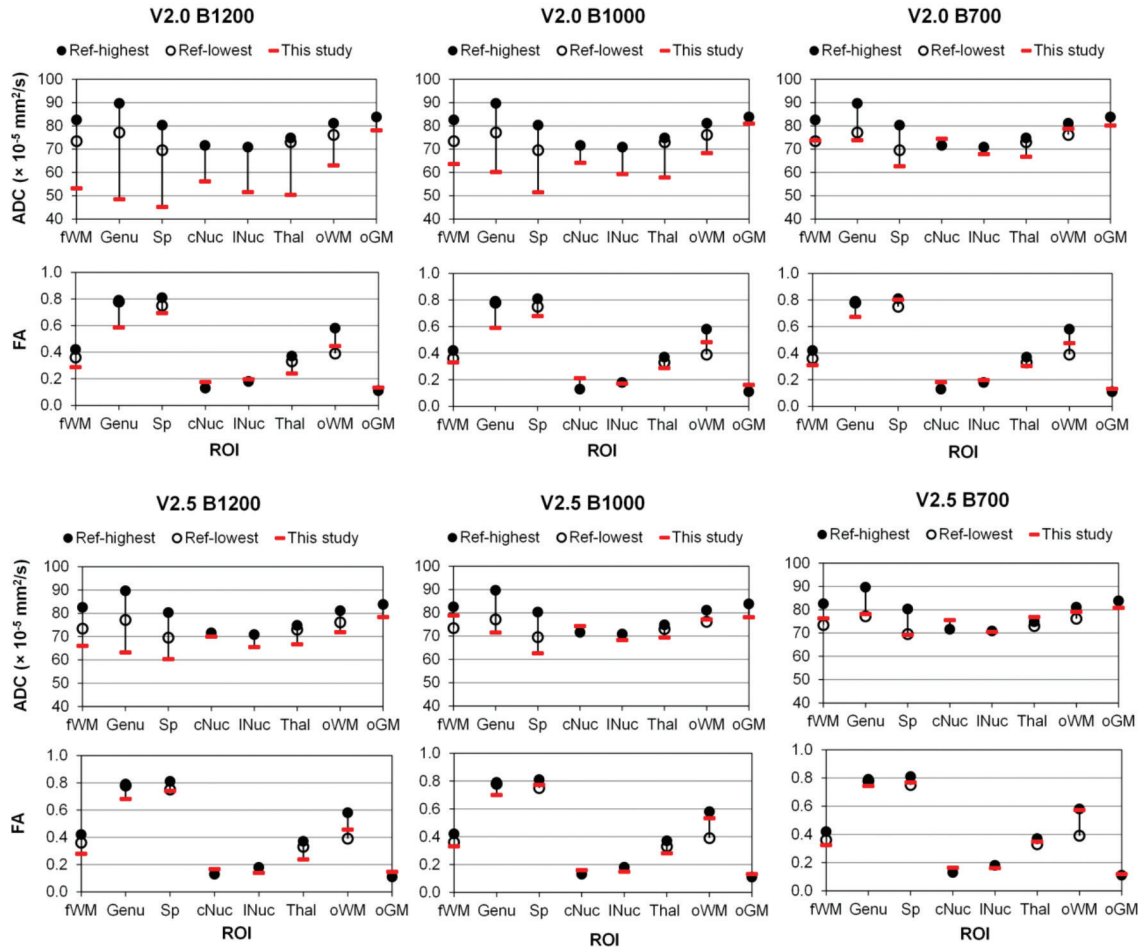
ᵃADC reported as MD in some of the articles referred. ᵇfWM: frontal white matter; Sp: splenium; cNuc: caudate nucleus; lNuc: lentiform nucleus; Thal: thalamus; oWM: occipital white matter; oGM: occipital grey matter. ᶜRef-highest: highest values in reference, Ref-lowest: lowest values in reference, This study: values obtained in this study

FIGURE 4. The ADCᵃ and FA values at all ROIsᵇ acquired for all of the protocolsᶜ

the SNR. However, since we do not have research level access to the MRI scanner in order to alter all imaging parameters, the RBW, g-factor and acceleration factor were kept constant according to vendor specification. The NEX were fixed to 1 as we aim to keep the scan time as minimum as possible. The TE became fixed by vendor to minimum value subject to b-value used whereas TR were fixed to 17 000 and 13 000 ms for voxel size 2.0 × 2.0 × 2.0 mm³ and 2.5 × 2.5 × 2.5 mm³, respectively, to allow coverage of whole phantom and brain. The number of diffusion direction was also fixed to 30, which is the minimum number required for robust estimation of tensor orientation and mean diffusivity as proposed by Jones (2004). Therefore, in the present study, only two parameters were varied, which are the voxel size (i.e. FOV, matrix and slice thickness) and b-value.

In terms of voxel size, we tried to obtain the smallest voxel size that could be achieved i.e. 2.0 × 2.0 × 2.0 mm³ while trying to compensate for an acceptable SNR and scan time. We chose isotropic voxel based on its advantages over non-isotropic voxels (Jones et al. 2002; Sasaki 2007;

Oouchi et al. 2007). We also chose the lowest and highest b-values (700 and 1200 s/mm², respectively) which were testified from previous work that those are the optimal b-value for brain imaging as well as the common b-value used, which is 1000 s/mm² (Bougias &Tripoliti 2009; Mori 2007; Mukherjee et al. 2008a).

ASSESSMENT OF SNR

This study has led to an understanding that the SNR improves with decreasing b-value and with increasing voxel size (Figure 1), which agrees well with the theory (Mukherjee et al. 2008b) and as predicted via (1) and (2). Our findings also matched with previous work on SNR assessment (Laganà et al. 2010; Lazar & Alexander 2003). It is also observed that modifications to the b-value, in our case it ranged from 200 to 500 s/mm², not much affect the SNR. On the other hand, an increase in voxel size of 0.5 × 0.5 × 0.5 mm³ showed SNR enhancement of approximately double. This indicates that the voxel resolution is a more dominating factor affecting the SNR compared to amount of diffusion weighting used.
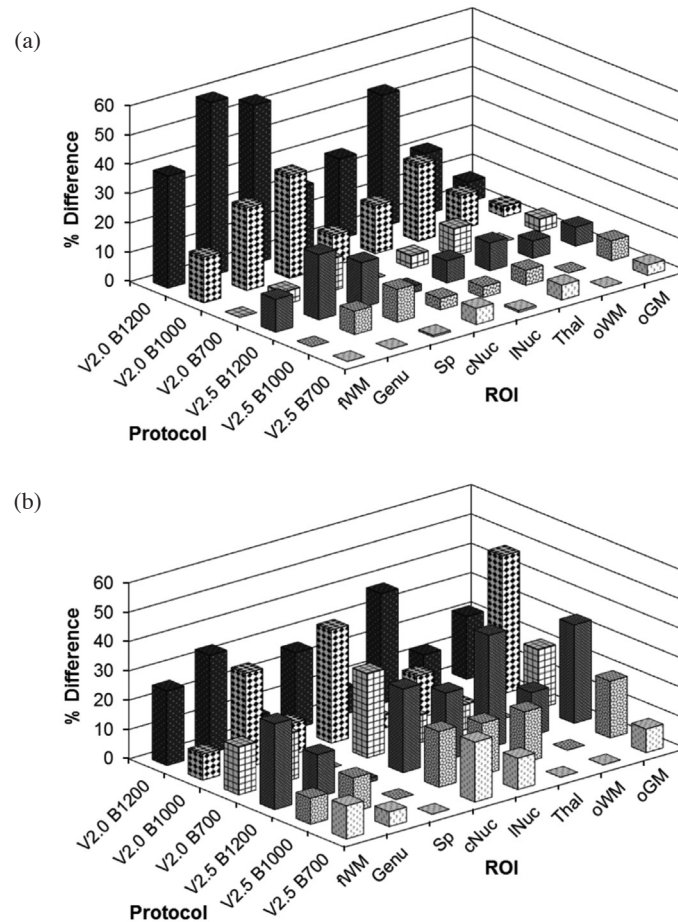
(a)

(b)

FIGURE 5. The percentage difference of (a) ADC and (b) FA values obtained
in this study as compared to references

It is noted that the SNR must be at least 20 to be considered as sufficient (Bastin et al. 1998; Mukherjee et al. 2008a). Our findings based on phantom study showed all protocols except protocols V2.0 B1200 and V2.0 B1000 provide sufficient SNR. However, measurement of SNR on CSF shows all protocols produce sufficient SNR (Figure 3). This is due to intrinsic characteristics of both phantom and CSF, in which CSF has higher water content, thus appeared more intense than phantom in the b_o images. Therefore, CSF exhibits SNR relatively higher than that of phantom for all protocols.

ADC AND FA VALUES

Influence of SNR on DTI values are also described well by our findings. This study showed that there is variation of ADC and FA value found from phantom measurement. Theoretically, the variation is due to two reasons. Firstly, the amount of diffusion weighting used in the protocol as described in (2) and secondly, bias in ADC and FA estimation caused by an insufficient SNR (Bastin et al. 1998; Mukherjee et al. 2008a).

Our findings showed that protocols with sufficient SNR displayed an insignificant increment of ADC value over smaller b-value. Thus it gives clue that V2.0 B1200 and V2.0 B1000 suffered from insufficient SNR (Figures 1 & 2). In this condition, our finding showed an agreement with a Monte Carlo simulation study which suggested that the ideal SNR is greater than 40 and SNR of less than 20 may results in underestimation of ADC and overestimation of FA (Bastin et al. 1998). A high FA noticed that in V2.0 B1200 does not at all represent the purely isotropic diffusion of the phantom. At the same time, a remarkably high standard deviation and variance of ADC and FA values between the three scans was also noted in V2.0 B1200 and V2.0 B1000 which indicates inconsistency of results (Figure 2).

It is also observed that protocols V2.0 B700 and V2.5 B700 displayed a comparable ADC values but different FA values as depicted in Figure 2. This result also reflects the effect of SNR on both of the protocols. Although the protocols exhibited sufficient SNR, however only V2.5 B700 achieved the ideal SNR as described above, thus it displayed smaller FA values.

Nonetheless, although all protocols with voxel 2.5 × 2.5 × 2.5 mm³ exhibited SNR of 40 and above, the smallest FA value that we could obtain was from protocol V2.5 B700. The FA value recorded is 0.0395 which is 3.95% deviated from the absolute FA value, i.e. zero. Besides

displaying small difference from absolute FA value, our results are comparable with that of obtained by Hunsche et al. (2001).

As can be seen from the *in-vivo* study (Figure 4), both ADC and FA values are affected by changes in b-value and voxel size. Our results for both phantom and *in-vivo* studies exhibited a similar trend for all of the protocols. Furthermore, the trend was also consistent with our findings on SNR where the most incomparable DTI values with references were noted in V2.0 B1200 and V2.0 B1000. This corresponds to the lowest and insufficient SNR obtained from phantom study. The effect is especially noticeable in the genu and splenium of the corpus callosum. Possible reason that explained this outcome is that insufficient SNR causes bias in estimating diffusion weighted signals. In case of high anisotropic white matter structure like corpus callosum, they are more greatly affected by insufficient SNR as the water diffusivity along the fibres orientation are less restricted. Thus, the diffusion weighted signals from this area are strongly attenuated, hence overestimated. Overestimation of the signals then leads to underestimation of ADC profile and anisotropy (Jones & Basser 2004; Mukherjee et al. 2008a). In our case, the ADC and FA value of genu and splenium were considerably deviated from previous findings (Figure 5).

Our finding demonstrates that protocols with voxel $2.5 \times 2.5 \times 2.5$ mm^3 give the required SNR. In terms of scan time, all of the protocols in this group took similar period to complete each scan which is 7.98 min. As can also be noted in Figures 4 and 5, among the three b-values, protocols V2.5 B1000 and V2.5 B700 displayed the most comparable results with references (Alexander & Barker 2005; Hunsche et al. 2001; Löbel et al. 2009) and only slight differences were noted between both protocols. Thus both protocols meet the requirement for brain imaging. However, when using b-value of 1000 s/mm^2, the scanner automatically reduces the limit of maximum number of slices allowable for data acquisition due to specific absorption rate (SAR) control. Instead, a protocol that could assure coverage of whole brain for all subjects are required to proceed with the next work on leukoaraiosis (Mohd Taib et al. 2012).

LIMITATIONS AND RECOMMENDATION FOR FUTURE WORK

In this research, no repetition has been done for *in-vivo* study due to two reasons. Firstly, the aim of *in-vivo* study was to validate the findings from the phantom study in which the phantom was scanned for three times. Thus, a single *in-vivo* scanning was reputed sufficient to achieve the objective of verifying the phantom study and that scan repetition is unnecessary. Secondly, the time taken to complete the entire scan is 52.03 min per session in which performing three times scan repetition on human subject is unpractical.

Besides that, single subject was used in this study and the results may not represent inter subject variability. However, our results from *in-vivo* study present a trend which is concordant with that of obtained from phantom study.

Despite all of the limitations mentioned previously, our findings gave the required information to understand the influence of parameters associated to DTI as well as to choose the best combination of parameters under consideration. Our next task is to study the inter subject variability using the optimum protocol obtained from this study and evaluate the range of DTI values produced by the MRI system.

CONCLUSION

Both phantom and *in-vivo* studies exhibited the similar trend of SNR values for all protocols. The finding demonstrated that protocols with voxel size of $2.5 \times 2.5 \times 2.5$ mm^3 give the desired SNR of at least 20. It was also found that a combination of voxel size of $2.5 \times 2.5 \times 2.5$ mm^3 with b-value of 1000 s/mm^2 (V2.5 B1000) and a combination of voxel size of $2.5 \times 2.5 \times 2.5$ mm^3 with b-value of 700 s/mm^2 (V2.5 B700) displayed the most agreeable results with the references. However, due to SAR limit, a compliant protocol that could assure the coverage of the whole brain for all subjects has to be selected accordingly. In conclusion, a combination of voxel size of $2.5 \times 2.5 \times 2.5$ mm^3 with b-value of 700 s/mm^2 were considered as an optimum parameters for brain DTI.

REFERENCES

Alexander, D.C. & Barker, G.J. 2005. Optimal imaging parameters for fiber-orientation estimation in diffusion MRI. *NeuroImage* 27(2): 357-367.

Bastin, M.E., Armitage, P.A. & Marshall, I. 1998. A theoretical study of the effect of experimental noise on the measurement of anisotropy in diffusion imaging. *Magnetic Resonance Imaging* 16(7): 773-785.

Bougias, C. & Tripoliti, E.E. 2009. Theory of diffusion tensor imaging and fiber tractography analysis. *European Journal of Radiography* 1(1): 37-41.

Chanraud, S., Zahr, N., Sullivan, E.V. & Pfefferbaum, A. 2010. MR diffusion tensor imaging: A window into white matter integrity of the working brain. *Neuropsychology Review* 20(2): 209-225.

Ding, X.Q., Finsterbusch, J., Wittkugel, O., Saager, C., Geobell, E., Fitting, T., Grzyska, U., Zeumer, H. & Fiehler, J. 2007. Apparent diffusion coefficient, fractional anisotropy and T2

relaxation time measurement: Does the field strength matter? *Clinical Neuroradiology* 17: 230-238.

Dietrich, O., Raya, J.G., Reeder, S.B., Reiser, M.F. & Schoenberg, S.O. 2007. Measurement of signal-to-noise ratios in MR images: Influence of multichannel coils, parallel imaging, and reconstruction filters. *Journal of Magnetic Resonance Imaging* 26 (2): 375-385.

Hunsche, S., Moseley, M.E., Stoeter, P. & Hedehus, M. 2001. Diffusion-tensor MR imaging at 1.5 and 3.0 T: Initial observations. *Radiology* 221(2): 550-556.

Jones, D.K., Lythgoe, D., Horsfield, M.A., Simmons, A., Williams, S.C.R. & Markus, H.S. 1999. Characterization of white matter damage in *Ischemic leukoaraiosis* with diffusion tensor MRI. *Stroke* 30(2): 393-397.

Jones, D.K. 2004. The effect of gradient sampling schemes on measures derived from diffusion tensor MRI: A Monte Carlo study. *Magnetic Resonance in Medicine* 51(4): 807-815.

Jones, D.K., Williams, S.C.R., Gasston, D., Horsfield, M.A., Sim, A. & Howard, R. 2002. Isotropic resolution diffusion tensor imaging with whole brain acquisition in a clinically acceptable time. *Human Brain Mapping* 15(4): 216-230.

Jones, D.K. & Basser, P.J. 2004. Squashing peanuts and smashing pumpkins: How noise distorts diffusion-weighted MR data. *Magnetic Resonance in Medicine* 52(5): 979-993.

King, K.F. 2004. ASSET - parallel imaging on the GE scanner. In *GE Healthcare* http://www.mr.ethz.ch/parallelmri04/abstracts/pub/King.pdf. Accessed on 22 December 2011.

Laganà, M., Rovaris, M., Ceccarelli, A., Venturelli, C., Marini, S. & Baselli, G. 2010. DTI parameter optimisation for acquisition at 1.5T: SNR analysis and clinical application. *Computational Intelligence and Neuroscience* 2010: 1-8.

Lazar, M. & Alexander, A.L. 2003. An error analysis of white matter tractography methods: Synthetic diffusion tensor field simulations. *NeuroImage* 20(2): 1140-1153.

Le Bihan, D., Mangin, J-F., Poupon, C., Clark, C.A., Pappata, S., Molko, N. & Chabriat, H. 2001. Diffusion tensor imaging: Concepts and applications. *Journal of Magnetic Resonance Imaging* 13(4): 534-546.

Löbel, U., Sedlacik, J., Güllmar, D., Kaiser, W.A., Reichenbach, J.R. & Mentzel, H.J. 2009. Diffusion tensor imaging: The normal evolution of ADC, RA, FA, and eigenvalues studied in multiple anatomical regions of the brain. *Neuroradiology* 51(4): 253-263.

Madden, D.J., Bennett, I.J. & Song, A.W. 2009. Cerebral white matter integrity and cognitive aging: Contributions from diffusion tensor iamaging. *Neuropsychology Review* 19: 415-435.

McRobbie, Donald W., Elizabeth A. Moore, Martin J. Graves, and Martin R. Prince. 2006. Chapter 5 - What you set is what you get: basic image optimization. In *MRI from Picture to Proton*, edited by McRobbie, D.W., Moore, E.A., G.M.J. & Prince, M.R. Cambridge: Cambridge University Press.

Mohd Taib, Nur Hartini, Wan Ahmad Kamil Wan Abdullah, Ibrahim Lutfi Shuaib, Enrico Magosso, & Suzana Mat Isa. 2012. Diffusion tensor imaging and tractography for the assessment of leukoaraiosis. Paper read at *IEEE EMBS Conference on Biomedical Engineering and Sciences (IECBES)*, 17-19 December 2012, at Langkawi, Malaysia.

Mori, S. 2007. Chapter 6 - Practical aspects of diffusion tensor imaging. In *Introduction to Diffusion Tensor Imaging*. Amsterdam: Elsevier Science B.V.

Mukherjee, P., Chung, S.W., Berman, J.I., Hess, C.P. & Henry, R.G. 2008a. Diffusion tensor MR imaging and fiber tractography: Technical considerations. *AJNR American Journal of Neuroradiology* 29: 843-852.

Mukherjee, P., Berman, J.I., Chung, S.W., Hess, C.P. & Henry, R.G. 2008b. Diffusion tensor MR imaging and fiber tractography: Theoretic underpinnings. *AJNR American Journal of Neuroradiology* 29: 632-641.

Oouchi, H., Yamada, K., Sakai, K., Kizu, O., Kubota, T., Ito, H. & Nishimura, T. 2007. Diffusion anisotropy measurement of brain white matter is affected by voxel size: Underestimation occurs in areas with crossing fibers. *AJNR American Journal of Neuroradiology* 28(6): 1102-1106.

Reeder, S.B., Wintersperger, B.J., Dietrich, O., Lanz, T., Greiser, A., Reiser, M.F., Glazer, G.M. & Schoenberg, S.O. 2005. Practical approaches to the evaluation of signal-to-noise ratio performance with parallel imaging: Application with cardiac imaging and a 32-channel cardiac coil. *Magnetic Resonance in Medicine* 54(3): 748-754.

Sasaki, M. 2007. High-resolution, isotropic-voxel acquisition technique improves quality and utility of diffusion-weighted and diffusion tensor imaging. *GE Healthcare Signa Pulse*. pp. 20-23.

Nur Hartini Mohd Taib & Wan Ahmad Kamil Wan Abdullah
Department of Radiology
School of Medical Sciences
Universiti Sains Malaysia
Kubang Kerian, Kelantan Darul Naim
Malaysia

Ibrahim Lutfi Shuaib, Enrico Magosso & Suzana Mat Isa
Advanced Medical and Dental Institute
Universiti Sains Malaysia
Kepala Batas, Pulau Pinang
Malaysia

*Corresponding author; email: nhartini@usm.my